Supplementary Materials

Experiment Section

The STM experiments were carried out in an ultrahigh vacuum (UHV) system (base pressure 1 $\times 10^{-11}$ mbar) equipped with a SPECS STM 150 Aarhus with SPECS 260 electronics. All the STM measurements were performed in constant current mode. A clean Cu(111) surface was prepared by cycles of sputtering with Ar^+ ions and annealing at 750 K, respectively. 4,4'-dihydroxydiphenyl (DOD) was purchased from commercial company, which was used without further purification. DOD molecules were vapor-deposited from a commercial Kentax evaporator with a Ta crucible held at 398 K (0.16 ML/min). The STM images were obtained after the substrate was cooled down below 100 K.

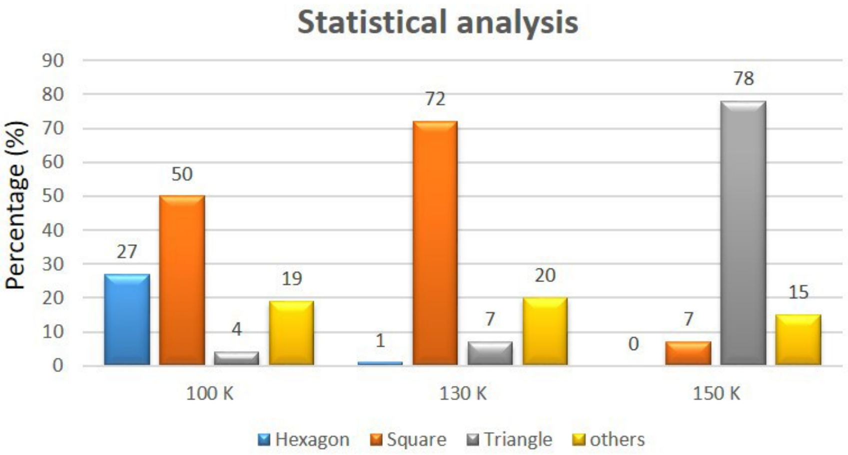

Fig. S1 Statistical analysis of the ratio of each molecular tessellation to whole supramolecular structure on Cu(111) at 100 K, 130 K, and 150 K, respectively, by counting more than 2,000 DOD molecules at every temperature point.

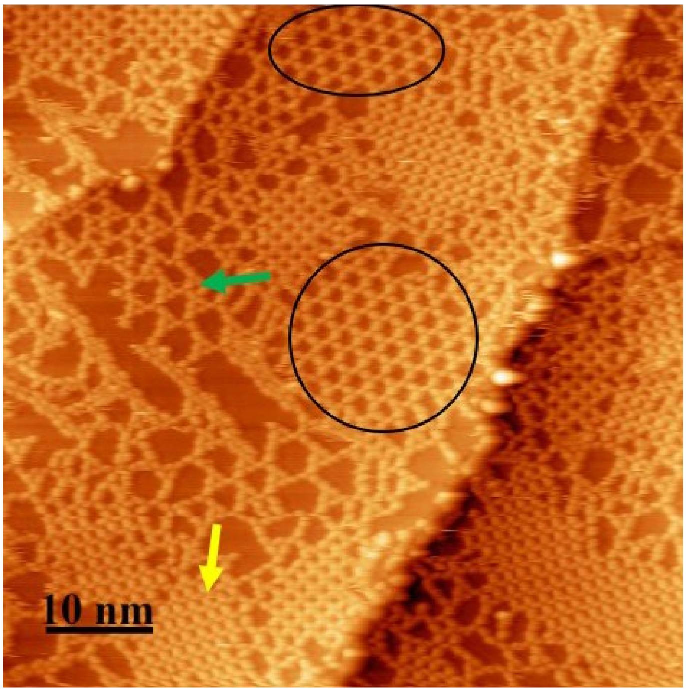

Fig. S2 Typical overview STM image recorded after deposition of DOD molecules on Cu(111) surface at 100 K. Hexagonal tessellations, square tessellations and triangular tessellations are marked by black circles, yellow and green arrows, respectively.

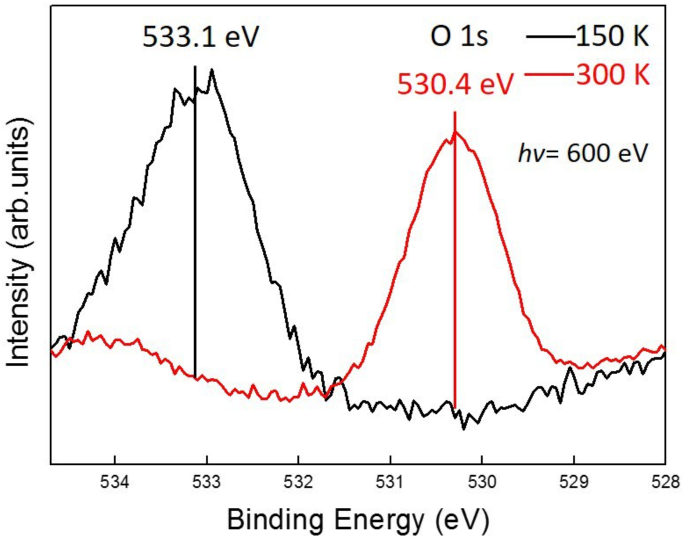

Figure S3. O 1s SRPES obtained after depositing 0.4 ML DOD onto Cu(111) surface held at 150 K and 300 K, respectively. The binding energy of O 1s 533.1 eV at 150 K (black peak), and 530.4 eV at 300 K (red peak). As reported previously,[1] the binding energy located at 533.1 eV is attributed to the terminal OH group of the intact DOD, and another one located at 530.4 eV, belongs to the generated C=O group after the dehydrogenation of the –OH. Because the substrate temperatures were below 150 K in out experiments, thus the DOD molecules in the three regular tessellations should keep intact.

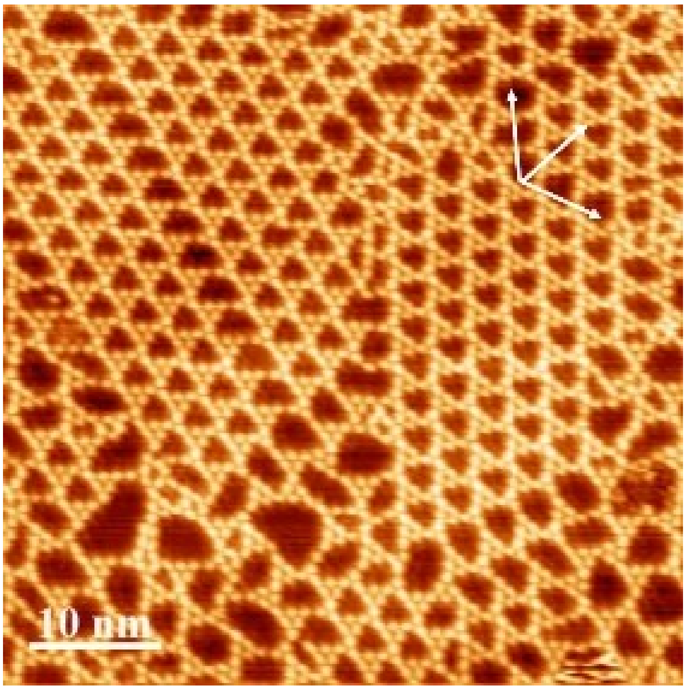

Fig. S4 Overview STM image of large-area chiral triangular regular tessellation on Cu(111) surface after annealing the sample as shown in Fig. 3 to 150 K.

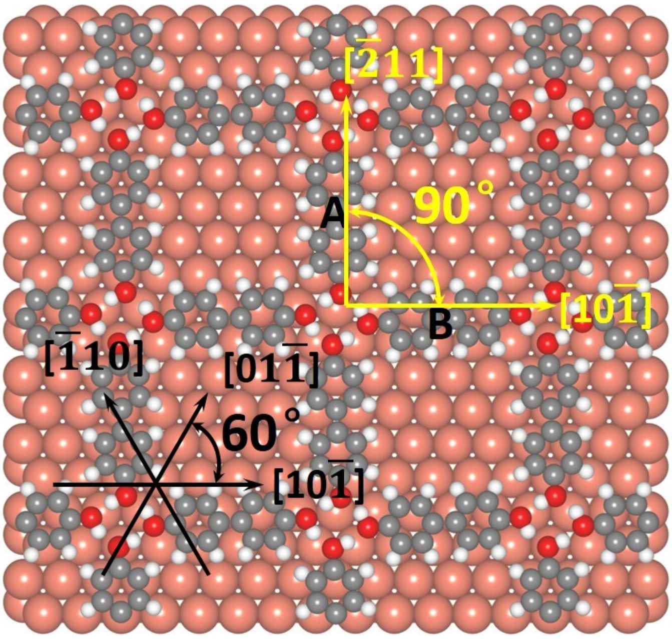

Fig. S5 Molecular model of the square tessellation. Molecule A and B are along with $[\bar{2}11]$ and $[01\bar{1}]$, respectively. Colour code: C, grey; H, white; O, red; Cu, pink.

Fig. S5 shows the molecular model of the square tessellation on the Cu(111) surface. Three high-symmetric directions of the Cu(111) surface are marked by black arrows. The axes of two-fold symmetric supramolecular network are along with $[01\bar{1}]$ and $[\bar{2}11]$ directions, respectively. The mismatch between the two-fold symmetry of supramolecular network and the three-fold symmetry of substrate leads to the different local chemical environments (different adsorbed sites) of the absorbed molecule A and B on the Cu(111). As a result, it leads the length and width of the formed square tessellation unequal.

DFT Calculations

All first principles calculations are performed by using density functional theory (DFT) method, implemented in Vienna Ab-initio Simulation Package (VASP)[2, 3] and adopting generalize gradient approximation (GGA) of Perdew-Burke-Ernzerhof (PBE) exchange-correlation functional[4]. Interactions between ions and electrons are approximated by the projector-augmented wave (PAW) potential[3, 5]. Van der Waals (vdW) corrections to the total energy are included by using the DFT-D3 method[6]. The cutoff energy for plane wave basis set is 400 eV. To simplify the simulation, two layer of Cu(111) surface with the bottom layer fixed at their bulk position is adopted with a total height of 20.0 Å and the Brillouin zone are sampled with Γ-centred2×2×1, 1×1×1 and 1×1×1 Monkhorst-Pack[7] k-points grid for hexagon, square and triangle configurations, respectively. The DOD/Cu(111) system is relaxed by keeping the bottom Cu atoms frozen and letting the upper Cu atoms and DOD molecules relax fully until the force is less than 0.05 eV/Å. The STM images simulations were carried out on the basis of Tersoff−Hamann theory and visualized using the p4VASP program[8, 9].

Table S1 Total binding energies of molecules per 100 nm^2 (E_{tb1}) and per molecule (E_{tb2}), energies of molecule-molecule interactions per molecule(E_{mol_mol}) and molecule-substrate interactions per molecule (E_{mol_sub}) and the number densities of molecules in theory (n_1) and experiment (n_2).

Structures	E_{tb1} (eV/100 nm^2)	E_{tb2} (eV/molecule)	$E_{mol\text{-}mol}$ (eV/molecule)	$E_{sub\text{-}mol}$ (eV/molecule)	n_1 (1/100 nm^2)	n_2 (1/100 nm^2)
Hexagon	-145.563	-2.163	-0.405	-1.758	67.294	71.833
Square	-240.432	-2.183	-0.601	-1.582	110.117	98.566
Triangle-ACW	-138.267	-2.067	-0.242	-1.826	66.881	64.523
Triangle-CW	-140.043	-2.094	-0.254	-1.840	66.881	64.523

They are evaluated by using the following equations,

$E_{tb1} = E_{sys} - n_2{*}E_{mol} - E_{sub}$ (1)

$E_{tb2} = E_{tb1}/n_2$ (2)

$E_{mol\_mol} = (E_{mol'} - n_2{*}E_{mol})/n_2$ (3)

$E_{mol\_sub} = (E_{sys} - E_{mol'} - E_{sub})/n_2$ (4)

where E_{sys} represents the total energy of the whole system per 100 nm^2, n_2 presents the number of DOD molecule per 100 nm^2, E_{mol} presents the energy of one freestanding DOD molecule, E_{sub} presents the energy of the relaxed substrate per 100 nm^2 and $E_{mol'}$ presents the energy of regular tessellation without Cu(111) substrate per 100 nm^2.

Discussions:

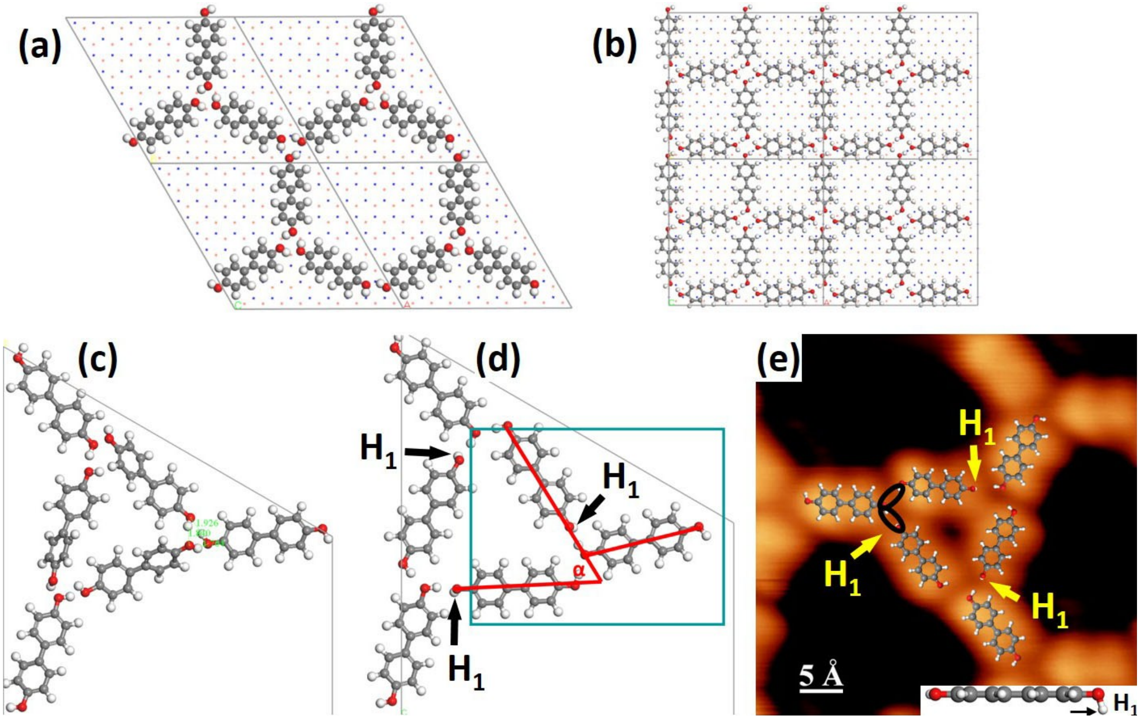

Fig. S7 (a), (b) The optimized structures of hexagonal and square molecular tessellations. (c) The most energy favored optimized model of ACW triangular structure, in which all hydrogen atoms of the hydroxyl groups take participate in the formation of hydrogen bonds. (d) The optimized structure of ACW triangular tessellation. (e) High-resolution STM image of the triangular structure, overlaid with molecular models.

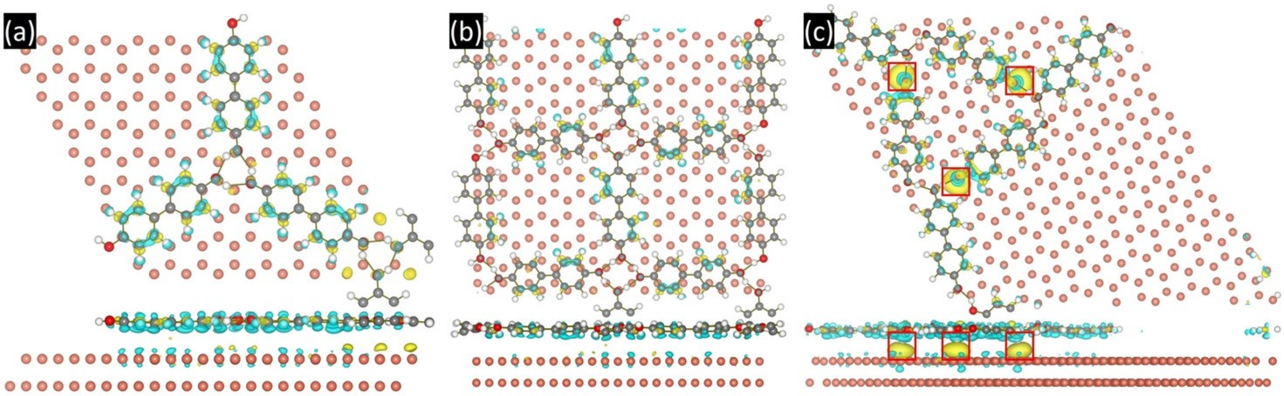

Fig. S8 The differential charge density (dρ) of the regular tessellation system was calculated according to the formula: dρ = ρ(system) - ρ(substrate)- ρ(pattern), where ρ(system) denotes the charge density of the whole system, ρ(substrate) denotes the charge density of the Cu(111) substrate removing DOD molecule without relaxation, ρ(pattern) denotes the charge density of regular tessellation removing Cu(111) substrate and keeping the molecules frozen. Differential charge densities with yellow and cyan colors represent positive and negative electron density isosurfaces, respectively. The value of isosurfaces is 0.0012 e/bohr^3. (a) Hexagonal molecular tessellation. (b) Square molecular tessellation. (c) ACW triangular molecular tessellation.

The optimized structures of a unitcell of hexagonal and square molecular tessellations are shown in Fig. S7a and Fig. S7b. Accordingly, three-fold and four-fold intermolecular hydrogen bonds are formed for the two cases, respectively. It can be seen that all hydrogen atoms of the hydroxyl groups take participate in the formation of hydrogen bonds in the two structures, which interact with the oxygen atoms of the adjacent molecules. The optimized structure of a unitcell of ACW triangular tessellation is shown in Fig. S7d. Differently, three hydrogen atoms as denoted as H_1 in Fig. S7d and Fig. S7e, do not take participate in the formation of hydrogen bonds. Therefore, six single-fold hydrogen bonds are involved within the hexamer cluster, as marked by black circles in Fig. S7e. As shown in Fig. S7d, the angle α between two neighboring DOD molecules is much smaller than 120° in the hexagonal tessellation and these two molecules are too close to each other. Strong repulsive force is existed between the H atom of the hydroxyl and the phenyl of these two molecules driving the H_1 atoms (as shown in Fig. S7d and Fig. S7e) move towards the substrate.

According to the DFT calculated results (table S1), the E_{tb2} values of the hexagonal and square molecular tessellations are -2.163 and -2.183 eV/molecule, respectively. The E_{tb2} value of square structure is lower than that of the hexagonal structure, indicating that square structure is the more thermodynamically stable. This is in agreement with the annealing-induced structure transformation from hexagonal to square molecular tessellations. The E_{tb2} value of the triangular molecular tessellation is -2.082 eV/molecule, higher than those of hexagonal and square tessellations. The result indicates that the triangular tessellation is thermodynamically unstable. Thus, the evolution from square to triangular structures should not be thermodynamically controlled process. Instead, we deduce that this process is most likely kinetically controlled. As stated above, the downward H_1 atoms may increase the interaction between molecule and substrate and restrict the diffusion of molecules on the surface. These limitations may make the transformation from triangular to square structure impossible. The irreversible transformation process is confirmed by our experiments. This deduction is supported by DFT-calculations. $E_{mol\text{-}sub}$ of the three molecular tessellations are calculated to be -1.758, -1.582 and -1.841 eV/molecule, respectively. The $E_{mol\text{-}sub}$ value of triangular structure is much lower than those of hexagonal and square structures, indicating the strong molecule-substrate interaction. Moreover, differential charge densities of the three structures further confirm the strong charge exchange between the H_1 atoms and the substrate in the triangular tessellation, as shown in Fig. S8. Overall, the transformation from hexagonal to square structures is thermodynamically controlled, while the transformation from square to triangular structure is most likely determined by on-surface kinetics.

Reference

1. Q. Li, B. Yang, H. Lin, N. Aghdassi, K. Miao, J. Zhang, H. Zhang, Y. Li, S. Duhm and J. Fan, *J. Am. Chem. Soc.*, 2016, **138**, 2809-2814.
2. G. Kresse and J. Furthmüller, *Phys. Rev. B*, 1996, **54**, 11169.
3. G. Kresse and D. Joubert, *Phys. Rev. B*, 1999, **59**, 1758.
4. J. P. Perdew, K. Burke and M. Ernzerhof, *Phys. Rev. Lett.*, 1996, **77**, 3865.
5. P. E. Blöchl, *Phys. Rev. B*, 1994, **50**, 17953.
6. S. Grimme, J. Antony, S. Ehrlich and H. Krieg, *J. Chem. Phys.*, 2010, **132**, 154104.
7. H. Monkhorst and J. Pack, 2005.
8. J. Tersoff and D. Hamann, *Phys. Rev. Lett.*, 1983, **50**, 1998.
9. J. Tersoff and D. Hamann, *Phys. Rev. B*, 1985, **31**, 805.